STM imagery and density functional calculations of C_{60} fullerene adsorption on the 6H-SiC(0001)-3×3 surface

T. Ovramenko,[1] F. Spillebout,[2] F. C. Bocquet,[3] A. J. Mayne,[1,*] G. Dujardin,[1] Ph. Sonnet,[2] L. Stauffer,[2] Y. Ksari,[3] and J.-M. Themlin[3]

[1]*Institut des Sciences Moléculaires d'Orsay, CNRS, UMR 8214, Université Paris Sud 11, 91405 Orsay, France*

[2]*Institut de Science des Matériaux de Mulhouse, CNRS UMR 7361, Université de Haute Alsace, 68093 Mulhouse, France*

[3]*Aix-Marseille Université, CNRS, IM2NP-UMR 7334, 13397 Marseille, France*

(Received 15 May 2012; revised manuscript received 25 February 2013; published 17 April 2013)

Scanning tunneling microscopy (STM) studies of the fullerene C_{60} molecule adsorbed on the silicon carbide SiC(0001)-3 × 3 surface, combined with density functional theory (DFT) calculations, show that chemisorption of individual C_{60} molecules occurs through the formation of one bond to one silicon adatom only in contrast to multiple bond formation on other semiconducting surfaces. We observe three stable adsorption sites with respect to the Si adatoms of the surface unit cell. Comprehensive DFT calculations give different adsorption energies for the three most abundant sites showing that van der Waals forces between the C_{60} molecule and the neighboring surface atoms need to be considered. The C_{60} molecules are observed to form small clusters even at low coverage indicating the presence of a mobile molecular precursor state and nonnegligible intermolecular interactions.

DOI: 10.1103/PhysRevB.87.155421 PACS number(s): 68.35.bp, 68.37.Ef, 68.43.Bc, 68.47.Fg

I. INTRODUCTION

Ever since their discovery,[1] fullerene molecules have generated great interest in their electronic[2] and structural properties.[3] This has led to many studies of fullerene adsorption on a number of metal[4,5] and semiconductor surfaces[6–8] using a variety of surface-sensitive techniques such as x-ray photoemission spectroscopy (XPS) and scanning tunneling microscopy (STM). Indeed, research on fullerenes remains a rich and active field,[9] as demonstrated by studies of ordered network formation on surfaces.[10–14] They can also be used to trap electrons[15] and act as cages to store atoms[16–18] or small molecules,[7,19–21] allowing the electronic properties (for example, conductivity) of the C_{60} to be tuned. Thus fullerenes are predicted[22] to make ideal candidates as building blocks in hybrid-molecular devices.[23,24] Advances in research towards possible applications in electronic devices have focused on the understanding of the binding mechanism of the C_{60} molecule to the metallic or semiconducting substrates already extensively used in the electronic industry.[25] It is known that C_{60} shows very particular adsorption behavior on different surfaces; for example, C_{60} binds to Si(100) via two or four Si-C bonds;[26–29] more bonds are formed at high temperature.[30,31] Similar behavior is observed on the Si(111) substrate,[32] where *ab initio* calculations show that charge transfer occurs following hybridization of the molecular orbitals with the surface states.[33,34]

Ideally, we would like C_{60} molecules adsorbed on a surface to retain their intrinsic molecular electronic properties. A rarely explored choice to electronically decouple the molecules from the surface is to use a wide band gap semiconductor. To achieve this, the gap of the semiconductor substrate should to be sufficiently large that the energy gap between the highest occupied molecular orbital (HOMO) and the lowest unoccupied molecular orbital (LUMO) of an organic molecule lies inside. Silicon carbide is a promising candidate for achieving electronic decoupling; with a wide indirect band gap of 3 eV, the SiC(0001)-3 × 3 surface reconstruction has no bulk electronic states over a broad energy range. Recent studies of the conjugated polyaromatic molecules H_2Pc[35] and PTCDI[36,37] show that these molecules bind to the SiC(0001)-3 × 3 surface via a Diels-Alder cycloaddition reaction through the formation of two Si-N and Si-O bonds, respectively. However, the SiC(0001)-3 × 3 surface has three intrinsic surface states located within the bulk band gap. Their physical morphology has a significant influence on the binding of molecules: The U_1-S_1 state is localized on the tetrahedral Si adatom pyramid, while the S_2 state is delocalized across the silicon adlayer. Two significant features, defining the adsorption character and electronic interaction of C_{60} with SiC surface, can be distinguished: (i) A large distance between neighboring Si adatoms reduces the ability to form multiple bonds, and (ii) the localized Mott-Hubbard surface states U_1 and S_1 induce strong electronic correlations which influence the surface electron transport.

Here, we present an STM study of C_{60} fullerenes adsorbed on the SiC(0001)-3 × 3 surface combined with density functional theory (DFT) calculations. The STM topographies show the presence of three stable adsorption configurations of C_{60} with respect to the adatoms of the surface unit cell, in contrast with earlier STM studies where only one adsorption configuration was observed and the nature of bonding was not discussed.[38,39] Our comprehensive DFT calculations show that individual C_{60} molecules are bonded to one silicon adatom via a single chemical bond. This is in contrast with multiple bond formation of C_{60} on other semiconducting surfaces.[24,25] Several variants of DFT were used to determine the adsorption energies for the three different configurations; a qualitative agreement with the statistical occurrence of each position was found. Both the STM studies and the DFT calculations indicate that the molecules are chemisorbed; however, the inclusion of van der Waals (vdW) forces between the C_{60} molecule and the neighboring surface atoms led to a significant increase in the calculated adsorption energy. While the vdW contribution per atom is small, it is additive and becomes significant when summed over all the atoms of the molecule. Finally,

the C_{60} molecules are observed in the STM images to form small clusters suggesting both a mobile precursor state before chemisorption and a nonnegligible intermolecular interaction.

II. EXPERIMENT AND THEORY

The room-temperature experiments were performed in an ultrahigh vacuum STM (Omicron GmbH) (base pressure 3×10^{-11} Torr) using electrochemically etched tungsten tips. A highly nitrogen-doped (density 3×10^{18} cm^{-3}) *n*-type 6H-SiC(0001) single crystal wafer was used. After outgassing, the SiC sample was flashed at 1100 °C to remove the native oxide, followed by silicon deposition on the surface at 650 °C for a few minutes,[40] giving a clear 3×3 LEED pattern indicating a well reconstructed surface.[41] The C_{60} fullerene molecules were evaporated on the clean SiC(0001)-3×3 surface using a Knudsen cell at 390 °C placed 4 cm in front of the sample. The exposure times were varied between 10 and 60 seconds.

The molecular adsorption configuration and electronic density of states were investigated by DFT calculations using the Vienna *Ab initio* Simulation Package (VASP) code.[42] We have compared the results from the general gradient approximation (GGA) operated alone within VASP with additional terms applied, namely, GGA with a spin polarization term (GGA + spin), and GGA plus a van der Waals term (DFT-D). The PW91 functional[43] and PAW pseudopotentials[44,45] were used with a plane-wave cutoff of 400 eV. The total energy in the DFT-D approach (noted $E_{\text{dft-d}}$) is given by $E_{\text{dft-d}} = E_{\text{dft}} + E_{\text{disp}}$ where E_{dft} is the usual self-consistent Kohn-Sham energy and E_{disp} is an empirical dispersion correction containing the C_6R^{-6} dependency used to simulate the vdW interactions.[46–48] The SiC(0001)-3×3 surface is modeled by a periodic slab of 3×3 unit cells composed of six atomic layers with 160 atoms in the unit cell and 60 atoms for the molecule. Due to the large size of slab (18.58 Å × 18.58 Å × 35 Å) only one Γ point is used. Increasing the number of layers involved in the slab does not modify the energetic order. The top four silicon layers were relaxed until the residual forces on the atoms were <0.02 eV/Å. Strong correlation effects are not included, so that the Mott-Hubbard surface states U_1 and S_1 are located at the Fermi level.

III. RESULTS AND DISCUSSION

A. Observations from the STM images

The STM images in Figs. 1(a) and 1(b) show C_{60} molecules adsorbed on the SiC(0001)-3×3 reconstructed surface. Individual molecules are seen as single protrusions about 13 Å in diameter. In the STM images, the isolated C_{60} molecules appear to be positioned differently with respect to the surface silicon adatoms. This contrasts with previous studies of C_{60} on the SiC surface,[38,39] where poor STM resolution prevented a detailed analysis of the adsorption sites, so the C_{60} molecules were thought to adsorb only on top of the Si adatoms. In our results, we observe three cases: (i) the bright spherical protrusion corresponding to the single C_{60} molecules sits symmetrically above (on top) a silicon adatom [Fig. 1(c), labeled "1"], (ii) the protrusion is positioned between two neighboring silicon adatoms [Fig. 1(d), labeled "2"], and (iii)

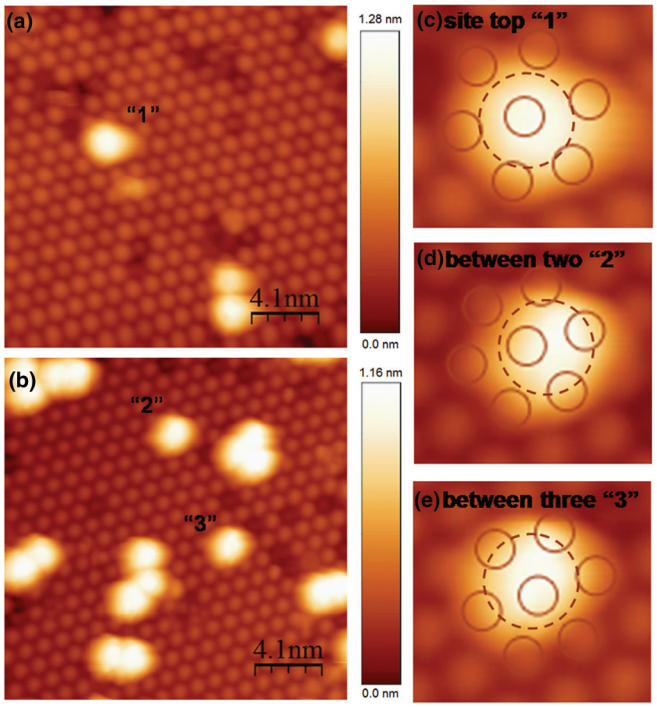

FIG. 1. (Color online) STM images and adsorption positions of C_{60} on the SiC(0001)-3×3 surface. (a), (b) Low-coverage 20.5 × 20.5 nm STM images of the C_{60} deposited on SiC(0001) [tunneling conditions: $U = -4$ V, $I = 0.5$ nA (a); $U = +2.5$ V, $I = 0.3$ nA (b)]. (c)–(e) Magnified views of three individual C_{60} molecules; the contours of Si adatom positions are marked by the small continuous circles (images size 2.5 × 2.5 nm); (c) C_{60} adsorbed on top (1), (d) C_{60} adsorbed between two Si adatoms (2), and (e) C_{60} adsorbed between three Si adatoms (3). Height scales are shown for (a), (c) and (b), (d), (e).

the protrusion is positioned between three silicon adatoms [Fig. 1(e), labeled "3"]. The sites (2) and (3) in Figs. 1(d) and 1(e) appear to be in different positions. However, thermal drift and tip effects introduce positional uncertainties in the images, which are evident if the two images are superimposed. This clearly prevents an immediate visual distinction in the molecular positions from being made. Therefore, a detailed and systematic statistical analysis of the high-resolution STM images is essential. The analysis (presented below) shows that single C_{60} molecules do indeed adsorb in three stable positions.

A series of 6 STM images in Fig. 2 illustrates the method used to determine the position of the C_{60} molecule with respect to the underlying Si adatoms. Using Photoshop (or similar image-treatment software), (a) choose the C_{60} to be analyzed by taking a zoom of Figs. 1(a), 1(b) select a small area of the clean SiC surface adjacent to the molecule in question, (c) the selected small area is made partially transparent and placed over the C_{60} molecule so that the adatoms overlap perfectly. (d) The small rectangle is made opaque to hide the molecule, (e) circles are then placed on the seven or so adatoms that are "under" the molecule so that the center of each circle is concentric with the center of each adatom; position error $< \pm 0.5$ Å. (f) Remove the small area so that the molecule is again visible leaving the circles in place indicating the adatom positions.

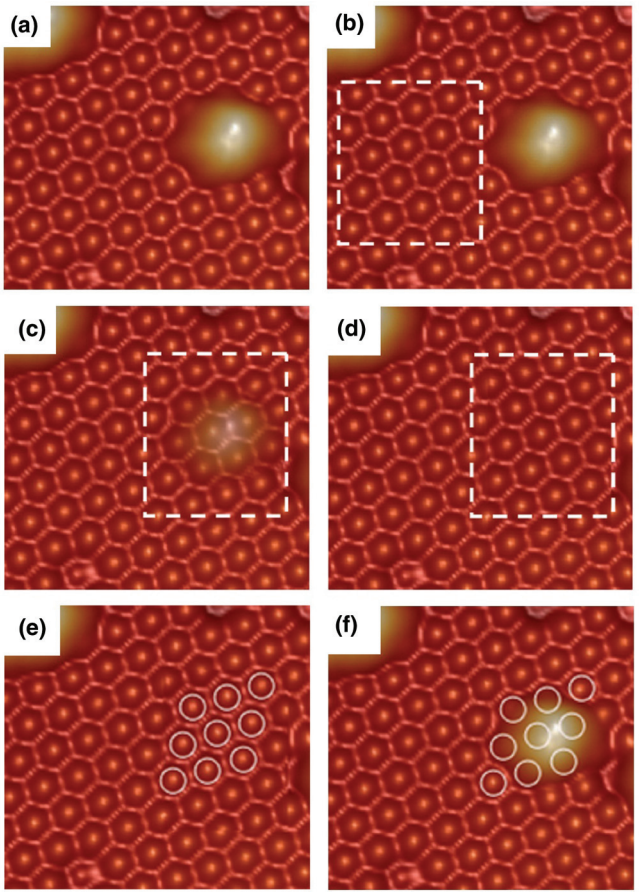

FIG. 2. (Color online) A series of six STM images illustrating the method used to determine the position of the C_{60} molecule with respect to the underlying Si adatoms. (a) Choose the C_{60} to be analyzed, (b) select a small area of the clean SiC surface adjacent to the molecule in question, (c) the selected small area is made partially transparent and placed over the C_{60} molecule so that the adatoms overlap perfectly. (d) The small rectangle is made opaque to hide the molecule, (e) circles are then placed on the seven or so adatoms that are "under" the molecule so that the center of each circle is concentric with the center of each adatom; position error ± 0.5 Å. (f) Remove the small area so that the molecule is again visible leaving the circles in place indicating the adatom positions. STM image size 8.5×8.5 nm, $U = +2.5$ V, $I = 0.3$ nA.

We now fit a large circle to the envelope of the C_{60} molecule. This is the most difficult part since the STM topography of the molecule may be influenced by the shape of the tip apex. Given the size of the C_{60} molecule, the tip can influence the topographic image of the molecule; if the tip apex is not circular in cross-section then the image of the C_{60} will be deformed. In addition, the DOS of the molecule is partly convoluted with the adatoms that are closest to the molecule, particularly those that are under the edge of the molecule. Since the molecules can be in different positions with respect to the underlying adatoms, this convolution deforms the outer envelope of the C_{60} so that it is neither conic nor circular. Any automated procedure which records the full width at half maximum contour would lead to the wrong result. This renders any automated procedure for determining the center almost impossible. Therefore, we determine the best fit by always considering the *same size* of circular contour and then by adjusting its position with the eye to fit the experimental topography. The circular contour has a diameter of 12.5 Å, which corresponds approximately to the envelope of the electron density around a C_{60} molecule. The *center* of the contour provides the position of each molecule with respect to the neighboring Si adatoms so that we can assign each adsorption site.

The results of the statistical analysis are presented in Fig. 3(a). The blue spots correspond to the positions of each of the 50 isolated C_{60} molecules relative to the Si pyramids (adatom + trimer). The x, y position of each spot was tabulated and the radial distance and angle with respect to the center Si adatom calculated. The distance of each blue spot from the central Si adatom is shown in Fig. 3(b). The distribution is bimodal with a first peak at around 1 Å (± 1 Å) and a second larger peak at about 4 Å (± 1 Å). The dotted circle (diameter 2.8 Å) encloses the 17 sites corresponding to the first peak while the 33 sites outside correspond to the second peak. Now, from the error in the position of the blue spot of about ± 1 Å (twice the diameter of the spot), we can estimate the error in the angular distribution to be about $\pm 5^\circ$. In Fig. 3(c), the reduced angular distribution is shown where the 360° distribution has been folded into a 60° segment with 5° bins. There are 33 molecules positioned outside the 2.8 Å circle of which 19 are preferentially located at $0^\circ \pm 10^\circ$ which correspond to the positions between two adatoms, and 14 at $30^\circ \pm 10^\circ$ which correspond to the positions between three adatoms. This clearly shows that there are distinct (2) and (3) configurations. Note that the 17 inside the dotted circle do not present any angular pattern. Returning to Fig. 3(a), we can attribute these 17 inside to the on-top position (1), the 19 at $0^\circ \pm 10^\circ$ modulo 60° to the (2) configuration, and the 14 at $30^\circ \pm 10^\circ$ modulo 60° to the (3) configuration.

B. DFT calculations

The STM images only give us information on the positions of the C_{60} molecules; *a priori* we can deduce neither the nature of the bonding to the surface nor the stability of the different sites from the adsorption energy values. As a result, we have performed comprehensive DFT calculations of the adsorption of a C_{60} molecule on the SiC(0001)-3×3 surface. In the VASP code a number of approximations can be implemented. In this study, we have modeled the possible adsorption sites using three different approximations: the general gradient approximation (GGA) alone, GGA with a spin polarization term (GGA + spin), and GGA with vdW forces included (DFT-D). The calculated relaxed adsorption configurations for the on-top (1), between two (2), and between three (3) positions are shown in Figs. 4(a), 4(b), and 4(c), respectively. The DFT calculations show (i) the formation of a simple covalent Si-C bond between a single Si adatom of the SiC surface and the C of the C_{60} molecule, and (ii) that the Si-C bond is found to tilt by 0°, 32°, and 36° with respect to the surface normal for adsorption positions (1), (2), and (3), respectively. These angles represent 3 local energy minima as a function of the tilt of the Si-C bond with respect to the surface normal. They are not necessarily the most stable in absolute terms, but it

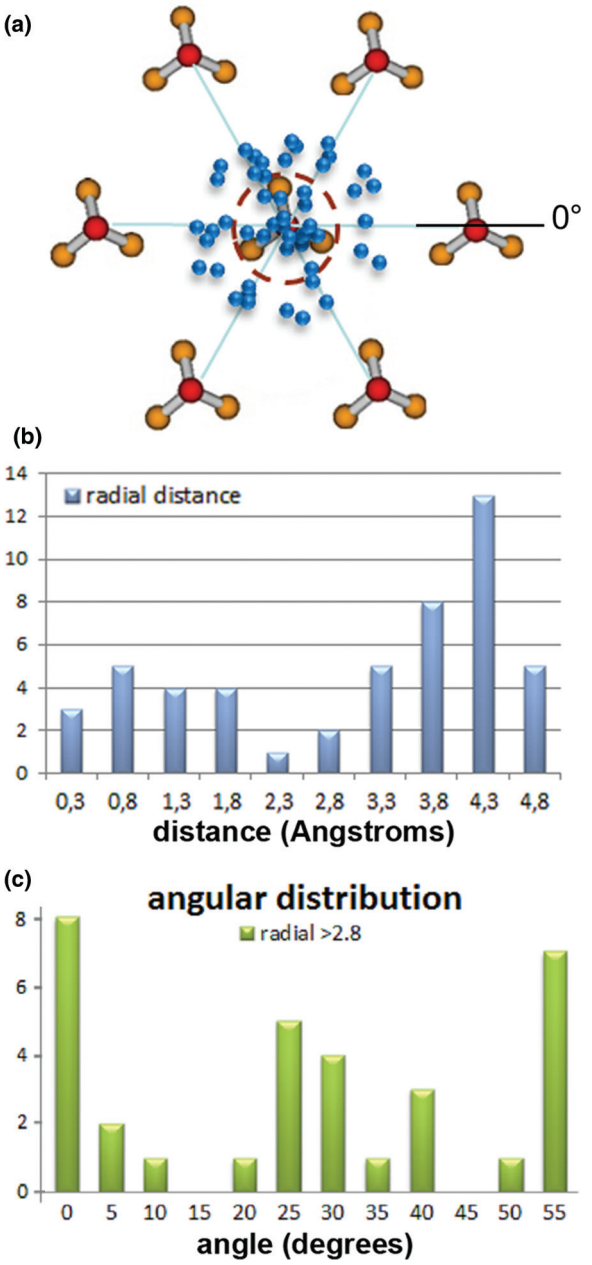

FIG. 3. (Color online) Statistical analysis of the positions of 50 isolated C_{60} molecules. (a) Schematic diagram showing the measured positions of the C_{60} molecules (blue spots) with respect to the Si adatom + trimer pyramids (red & orange tripods) of the SiC(0001)-3×3 surface. The estimated position error of ± 1 Å is twice the diameter of each blue spot. The dotted brown circle has a radius of 2.8 Å. (b) The radial distribution of the molecular positions from the center Si adatom. (c) Angular distribution over 360° is folded into a 60° segment in 5° bins, for the positions outside the 2.8 Å circle.

is not possible to search the entire potential energy surface, and we do not know the energy barriers to adsorption. The adsorption energies, relaxed tilt angle, and Si-C bond length, extracted from the calculations, are presented in Table I for the three adsorption conformations (1), (2), and (3). For a bond tilt towards a neighboring adatom [configuration (2)] one could expect *a priori* the formation of a second Si-C bond

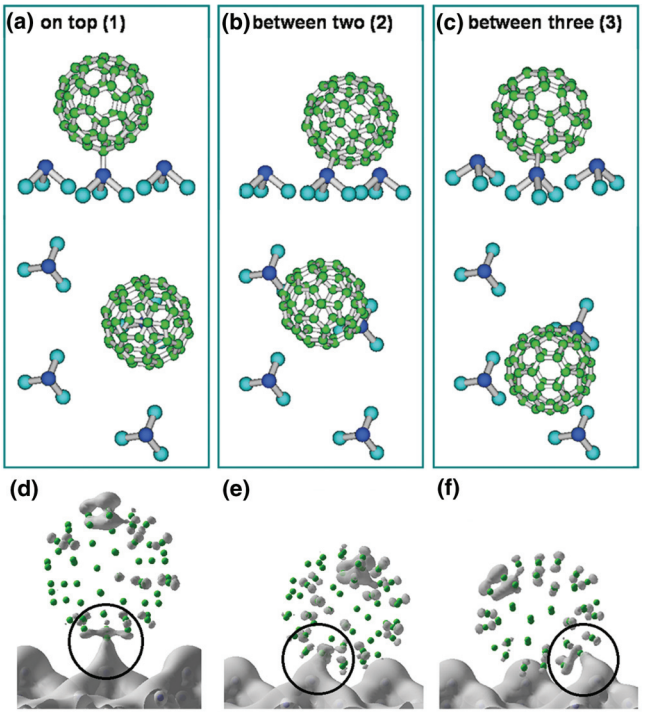

FIG. 4. (Color online) Calculated ball and stick structure of the C_{60} molecule on the SiC surface. Top and side views of a single C_{60} molecule positioned (a) on top (1), (b) between two (2), and (c) between three (3). In the schematic diagrams, only the Si pyramid atoms of the SiC(0001) reconstruction are shown underneath the C_{60} molecule. (d)–(f) Isodensity maps of the C_{60} molecule on the SiC surface for the energy range of -3.5 to -3.0 eV (isodensity = 0.028 $e^-/\text{Å}^3$) showing the density of states associated with the Si-C bond (black circles) for (d) the on-top (1), (e) between two (2), and (f) between three (3) sites.

with the neighboring Si adatom towards which the molecule is facing. However, the calculations indicate that forming two Si-C bonds is energetically unfavorable because the Si-Si adatom separation is large (9.28 Å). Indeed, if the calculations are initiated with two Si-C bonds, one bond is observed to break during the relaxation of the system. Tilting the Si-C bond reduces the orbital overlap between the p_z dangling bond of the Si adatom and the p_z orbital of the bonding carbon atom of the C_{60} cage, increasing the bond length slightly from 2.00 to 2.17 Å. A small deformation of the cage takes places where the binding C atom undergoes a change in hybridization from sp^2 to sp^3. Indeed, the DFT calculations show that the new Si-C bonding orbital is located in the energy range from -3.0 eV to -3.5 eV. The isodensity maps for the three sites (on top, between two, and between three), plotted in Figs. 4(d)–4(f), clearly show the electron density associated with the new Si-C bond between the Si adatom and the C_{60} molecule (dotted circles).

The third aspect concerns the calculated values of the adsorption energies. The GGA and GGA + spin calculations give similar negative adsorption energies; the most stable configuration is the on top (1) while the (2) and (3) sites are less strongly bound, in contrast with the statistical frequency of occurrence of each position determined from the experiment.

TABLE I. Adsorption energies and Si-C bond angles and bond lengths for a single C_{60} molecule adsorbed on the SiC(0001)-3 × 3 surface.

C_{60} position	No. molecules (%)	GGA (E_{ads}, eV)	GGA + spin (E_{ads}, eV)	GGA + vdW (E_{ads}, eV)	SiC angle (°)	SiC length (Å)
(1)	17 (34 ± 8%)	− 0.73	− 0.67	− 1.22	0	2.00
(2)	19 (38 ± 9%)	− 0.44	− 0.23	− 1.43	32	2.07
(3)	14 (28 ± 7%)	− 0.30	− 0.21	− 1.57	36	2.17

However, inclusion of a vdW term dramatically changes the results of the calculation; not only is the absolute binding energy increased but more importantly, the order is completely reversed (in terms of more or less stable configurations). The (3) configuration is now the most stable (− 1.57 eV) and the on-top (1) configuration the least (− 1.22 eV). The adsorption energies for configurations (2) and (3) differ by 0.15 eV, which is small but not negligible,[36,37] because the differences between the sites (2) − (1) and (3) − (1) are only 0.21 and 0.36 eV, respectively. Using Grimme's approach,[46–48] the calculated vdW energy contribution is not small. This has already been observed in several cases: molecules on an Au(111) surface,[49] supported supramolecular networks,[50] or a supramolecular network on graphite.[51] A covalent bond interaction between two atoms is stronger than a vdW interaction between two atoms. However, the vdW energy is additive; per atom the vdW contribution is small but it becomes significant when summed over all the atoms of the molecule. Indeed, Mura *et al.*[49] have shown a relationship between the binding energy of three different molecules and the number of atoms within each molecule. In the C_{60} molecule, the large number of carbon atoms explains why the vdW energy is not small in contrast to what we could expect. Our calculations show that the vdW contribution is 0.49, 0.99, and 1.27 eV, while the covalent energy (corresponding to the GGA approximation alone) decreases strongly: 0.73, 0.44, and 0.30 eV for the (3), (2), and (1) positions, respectively. It is evident that the vdW interactions are not negligible. As stated above, there is no direct bonding with the neighboring adatom in the (2) and (3) conformations. Indeed, if a C_{60} molecule was initially adsorbed on the surface without any Si-C bond, in the framework of the DFT-D approximation, the relaxation of the system led to the creation of one Si-C bond.

A single bond between the C_{60} and the SiC surface is not favorable from an electronic point of view because it leads to the formation of a partial positive charge localized on the C_{60} molecule. Intuitively, an electron from the Si adatom dangling bond combines with an electron from a p_z orbital of one of the C_{60} carbon atoms to form the Si-C bond. Consequently, the C_{60} molecule has an effective positive charge which is compensated (at least partially) by an electron from the surface. Charge transfer from the surface to the molecule is also observed for C_{60} on a metal surface,[25] on Si(111),[34] and for other organic molecules on SiC.[36,37] In Fig. 5(a), our calculated density of states (DOS) of the adsorbed C_{60} molecule in configuration (3) (orange spectrum) shows the existence of a peak at the Fermi level (arrow) compared to the free molecule (blue spectrum). We can estimate the degree of charge transfer by measuring the area of the DOS peak of the adsorbed C_{60} molecule that is just below the Fermi level (i.e., from − 0.35 to 0 eV); we find 0.76, 0.81, and 0.68 electrons for the (1), (2), and (3) positions, respectively. Further examination of Fig. 5(a) reveals the presence of additional peaks in the calculated DOS that are not present in the gas phase spectrum. As already postulated for C_{60} adsorption on Si(111)-7 × 7,[34] it is the complex hybridization between the molecular orbitals and the surface states that is responsible for the charge transfer rather than a direct transfer into the LUMO. The isodensity map of the (3) configuration is presented in Figs. 5(b) and 5(c), with the clean surface for comparison in Fig. 5(d). It is evident from Fig. 5 that the molecular orbitals involved in the bonding show a complex spatial dependence. For the peak close to E_F, our DFT results reveal that the electron density is partially delocalized over the C_{60} molecule and that the electron density on the Si adatom pyramid is absent. No experimental scanning tunneling spectroscopy is shown here, because $I(V)$ spectroscopy of molecules on the SiC surface is very difficult to perform and analyze, especially at low voltage close to the Fermi level due to the wide band gap of SiC substrate.[36]

Inverse photoemission spectroscopy (IPES) experiments[52] reveal additional information confirming the chemisorption of C_{60} on the SiC surface. Spectra taken as a function of temperature show that C_{60} molecules desorb intact from the 3 × 3 surface in stark contrast to the molecular cage

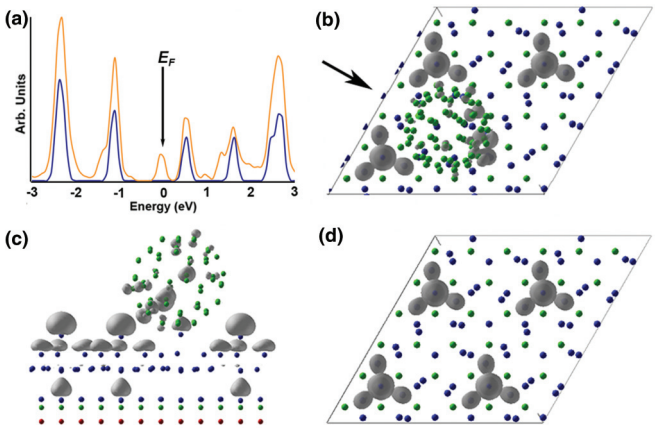

FIG. 5. (Color online) (a) DFT calculations of the density of states for the entire C_{60} molecule in the gas phase (blue) and adsorbed (orange) between − 3 and + 3 eV. (b) Isodensity map of the C_{60} molecule on the SiC surface [in configuration (3)] within the energy window from − 0.35 to 0 eV (isodensity = 0.028 $e^-/Å^3$). This corresponds to the peak at E_F marked in (a). (c) Same isodensity map as in (b) as viewed from the side; the arrow in (b) indicates the direction of vision. (d) Isodensity map of the clean SiC surface in the same energy range as (b) and (c) (isodensity = 0.028 $e^-/Å^3$).

opening observed on the $\sqrt{3} \times \sqrt{3}$ SiC surface, or indeed other substrates such as Si(111) and Si(100).[52] The fact that cage opening is not observed on the 3×3 surface is another indication of single Si-C bond formation.

C. Spatial coverage and statistics

We now consider the adsorption of C_{60} from another perspective; at low coverage, the C_{60} molecules appear to form small clusters as observed in the STM images in Fig. 6. Four experiments, presented in Table II, were made on four different samples with exposure times of 10, 20, 30, and 60 seconds, resulting in coverages of 1.7, 5.4, 5.3, and 12.3 %, respectively. Two methods can be used to determine statistically whether the spatial distribution of adsorbed clusters is random. The first method[53] compares the distribution of the cluster sizes with the expected values for each size of cluster. This probabilistic model considers that for an array of adsorption sites, each site can be occupied by only one molecule, and that the adsorption on one site is independent of any other site. This method has been applied to small molecules such as ethylene on Si(100)[54] and oxygen on Si(100).[55] We can apply this method to study the C_{60} adsorption on SiC because only one C_{60} molecule can fit in a surface unit cell. Indeed, we define the fractional coverage (or density) of molecules as f = number of C_{60} molecules divided by the number of unit cells in the STM image; f is then normalized to a standard image size. In this statistical method, we define the probability P_1 of finding a single molecule M_1 as the conditional probability that a neighboring adsorption site is empty given that the first site is occupied by a molecule. If we consider that the placement of molecules and empty sites is random, that is, they are independent, then P_1 is the probability that the site is empty, given by $P_1 = (1 - f)$, where f is the fractional coverage (or density) of molecules, assuming one molecule per unit cell. A cluster of two molecules, M_2 is then $P_2 = P(\text{empty}) \times P(\text{molecule}) = (1 - f)f$. Thus a cluster M_n has the probability $P_n = (1 - f)f^{n-1}$. The 30×30 nm STM image in Fig. 6(a), obtained after a 20 s exposure, contains 49 molecules (second line in Table II). We count 11 isolated C_{60} molecules, 6 clusters containing two molecules, 5 clusters containing three molecules, 1 cluster containing 4 molecules, and 1 cluster containing 7 molecules. For the same coverage density ($f = 0.054$) we would expect 46 isolated molecules and 3 clusters containing two molecules (the expected values are in parentheses in Table II). While it is clear that there are fewer single molecules and more large clusters than would be expected for a random distribution, attributing each molecule to a cluster is not easy.

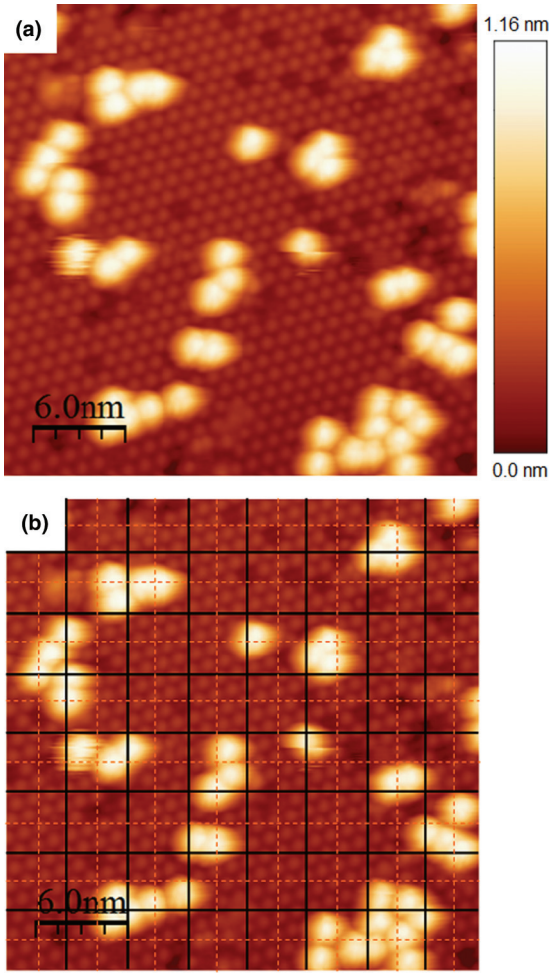

FIG. 6. (Color online) STM images of the C_{60} molecules showing clustering at low coverage. (a) 30×30 nm STM topography showing individual C_{60} molecules and clusters [tunneling conditions: -3 V, 0.3 nA; height scale is given for (a) only as (b) is identical]. (b) The same image as in (a) overlaid by a square grid. Two different grid sizes were used; the first contains 64 squares of 3.75×3.75 nm, while second one contains 256 squares, each 1.88×1.88 nm.

The second method using a Poisson distribution of a discrete random variable provides a more robust analysis. Typically, this statistical distribution is formed by the number of events that occur in a certain spatial interval. This method is applicable to a surface analysis by considering that the distribution is spatial; in this case, the STM image is divided into squares. For each image a grid is placed over the STM image and the number of molecules in each grid

TABLE II. An analysis of the number of different sized C_{60} molecular clusters (M) as a function of exposure time.

Exposure (time, s)	No. molecules (30×30 nm)	Coverage (fraction)	Clusters				
			M_1	M_2	M_3	M_4	$\geqslant M_5$
10	15	0.017	3(15)[a]	2(0)	1(0)	0(0)	1(0)
20	49	0.054	11(46)	6(3)	5(0)	1(0)	1(0)
30	48	0.053	14(46)	5(2)	4(0)	3(0)	0(0)
60	111	0.123	21(97)	6(12)	7(2)	4(0)	6(0)

[a]Numbers in parentheses correspond to the expected values.

TABLE III. A 2D Poisson distribution analysis of the number of C_{60} molecules, as a function of exposure time, using a 64-square grid.

Exposure (time, s)	$N/64$ (λ)	χ	Grid square occupancy					
			$k=0$	$k=1$	$k=2$	$k=3$	$k=4$	$k=5$
10	0.23	19.1	55(51)[a]	4(12)	4(1)	1(0)	0(0)	0(0)
20	0.77	23.0	38(30)	11(23)	10(9)	3(2)	1(0)	1(0)
30	0.75	14.6	38(30)	10(23)	10(9)	6(2)	0(0)	0(0)
60	1.73	17.7	17(11)	19(20)	9(17)	6(10)	9(4)	4(1)

[a]Numbers in parentheses correspond to the expected values.

cell is counted.[56] The Poisson distribution is defined as the probability that the random values do not exceed some given value k, which is given by $P(k) = e^{-\lambda}(\lambda^k/k!)$,[57] where λ is the average number of molecules per square. Thus, if $P(k)$ is multiplied by the number of squares, the expected number of squares containing k molecules is obtained. Considering again the same 30×30 nm STM image [Fig. 6(b)] with 49 molecules after a 20 s exposure, we count the occupation or not of the grid squares. For 64-grid cells, the results presented in Table III show that 38 are empty, 11 contain a single C_{60} molecule, 10 grid squares contain two molecules, 3 contain three molecules, 1 contains four molecules, and 1 contains 5 molecules. The expected Poisson distribution values are given in parentheses in Table III and predict 30 empty squares, 23 squares with one molecule, 9 with two molecules, and 2 squares with 3 molecules. To ensure consistency over different length scales, the analysis was repeated using a grid of 256 squares (Table IV), and the same behavior is observed. This analysis clearly shows that there are more empty squares and fewer single molecules as well as more clusters than expected for a random distribution.

Our statistical analyses of the STM images using two different methods show that the C_{60} molecules form clusters even at low coverage, implying an attractive intermolecular interaction. Now, a simple tilting of the SiC bond is not sufficient to explain this interaction. Indeed, an analysis of the position of the C_{60} molecules, inside the small clusters of two and three molecules, revealed that all combinations were possible: 11, 12, 13, 23, etc; there is no preference. It should be mentioned that the analysis of the adsorption position inside a cluster has a higher uncertainty than for individual molecules. This tendency to form clusters could be explained by a physisorbed precursor state prior to chemisorption. In addition, the formation of a polarized Si-C bond and the charge transfer to the C_{60} molecules could modify the reactivity of neighboring adsorption sites,[58] or reduce energy of the barrier to chemisorption in the vicinity of an already adsorbed C_{60} molecule.[59]

IV. CONCLUSIONS

In conclusion, STM studies combined with density functional theory (DFT) calculations show the presence of three stable adsorption sites for the isolated molecule with respect to the adatoms of the SiC(0001)-3×3 surface unit cell. This is in contrast with earlier STM studies where only one adsorption configuration was observed. Furthermore, the DFT calculations show that individual C_{60} molecules are bonded to one silicon adatom via a single chemical bond in contrast to multiple bond formation on other semiconducting surfaces. The comprehensive DFT calculations with and without spin polarization and van der Waals terms give different adsorption energies for the 3 different configurations. It is important to note that the configurations with a tilted Si-C bond are energetically more favorable, showing that the van der Waals forces between the C_{60} molecule and the neighboring surface atoms need to be considered. Only 34% of the molecules adsorb in the "on top" configuration, while 66% of the molecules undergo a significant tilt. Finally, in the STM images, the C_{60} molecules show a clear tendency to form small clusters suggesting both a mobile precursor state before chemisorption and a nonnegligible intermolecular interaction.

ACKNOWLEDGMENTS

We would like to thank the referee for constructive comments. This work was supported by the ANR project MolSiC (Contract No. ANR-08-NANO-058). This work was performed using HPC resources from GENCI-IDRIS (Grant No. 2010-096459) and computations have also been performed on the supercomputer facilities of the Mésocentre de Calcul de Franche-Comté.

TABLE IV. A 2D Poisson distribution analysis of the number of C_{60} molecules, as a function of exposure time, using a 256-square grid.

Exposure (time, s)	N/256 (λ)	χ	Grid square occupancy				
			$k=0$	$k=1$	$k=2$	$k=3$	$k=4$
10	0.06	118	245(241)[a]	8(14)	2(1)	1(0)	0(0)
20	0.19	4.5	215(211)	34(41)	6(4)	1(0)	0(0)
30	0.19	14.1	219(212)	27(40)	9(4)	1(0)	0(0)
60	0.43	3.8	171(166)	64(72)	17(15)	3(2)	1(0)

[a]Numbers in parentheses correspond to the expected values.

*Email address: andrew.mayne@u-psud.fr

[1] H. W. Kroto, J. R. Heath, S. C. O'Brien, R. F. Curl, and R. E. Smalley, Nature (London) **318**, 163 (1985).

[2] H. W. Kroto, Rev. Mod. Phys. **69**, 703 (1997).

[3] H. W. Kroto, R. Taylor, and D. R. M. Walton, Pure Appl. Chern. **66**, 2091 (1994).

[4] M. Grobis, A. Wachowiak, R. Yamachika, and M. F. Crommie, Appl. Phys. Lett. **86**, 204102 (2005).

[5] N. A. Pradhan, N. Liu, and W. Ho, J. Phys. Chem **109**, 8513 (2008).

[6] J. G. Hou, Y. Jinlong, W. Haiqian, L. Qunxiang, Z. Changgan, L. Hai, B. Wang, D. M. Chen, and Z. Qingshi, Phys. Rev. Lett. **83**, 3001 (1999).

[7] D. L. Keeling, M. J. Humphry, R. H. J. Fawcett, P. H. Beton, C. Hobbs, and L. Kantorovich, Phys. Rev. Lett. **94**, 146104 (2005).

[8] D. L. Keeling, M. J. Humphry, P. Moriarty, and P. H. Beton, Chem. Phys. Lett. **366**, 300 (2002).

[9] P. J. Moriarty, Surf. Sci. Rep. **65**, 175 (2010).

[10] G. Schull and R. Berndt, Phys. Rev. Lett. **99**, 226105 (2007).

[11] J. A. Theobald, N. S. Oxtoby, M. A. Phillips, N. R. Champness, and P. H. Beton, Nature (London) **424**, 1029 (2003).

[12] X. Zhang, W. He, A. Zhao, H. Li, L. Chen, W. W. Pai, J. Hou, M. M. T. Loy, J. Yang, and X. Xiao, Phys. Rev. B **75**, 235444 (2007).

[13] G. Schull, N. Néel, M. Becker, J. Kroger, and R. Berndt, New J. Phys. **10**, 065012 (2008).

[14] M. Nimmrich, M. Kittelmann, P. Rahe, W. Harneit, A. J. Mayne, G. Dujardin, and A. Kühnle, Phys. Rev. B **85**, 035420 (2012).

[15] T. Matsushima, M. Yahiro, and C. Adachi, Appl. Phys. Lett. **91**, 103505 (2007).

[16] P. J. Benning, José Luis Martins, J. H. Weaver, L. P. F. Chibante, and R. E. Smalley, Science **252**, 1417 (1991).

[17] Y. Yasutake, Z. Shi, T. Okazaki, H. Shinohara, and Y. Majima, Nano Lett. **5**, 1057 (2005).

[18] A. Strozecka, K. Muthukumar, A. Dybek, and T. J. Dennis, Appl. Phys. Lett. **95**, 133118 (2009).

[19] D. S. Deak, F. Silly, K. Porfyrakis, and M. R. Castell, Nanotechnology **18**, 075301 (2007).

[20] T. Korona and H. Dodziuk, J. Chem. Th. Comp. **7**, 1476 (2011).

[21] S. Stevenson, G. Rice, T. Glass, K. Harich, F. Cromer, M. R. Jordan, J. Craft, E. Hadju, R. Bible, M. M. Olmstead, and K. Ma, Nature (London) **401**, 55 (1999).

[22] W. Harneit, Phys. Rev. A **65**, 032322 (2002).

[23] J. Twamley, Phys. Rev. A **67**, 052318 (2003).

[24] S. Schaefer, K. Huebener, W. Harneit, C. Boehme, K. Fostiropoulos, H. Angermann, J. Rappich, J. Behrends, and K. Lips, Solid State Sci. **10**, 1314 (2008).

[25] G. Schull, T. Frederiksen, A. Arnau, D. Sánchez-Portal, and R. Berndt, Nat. Nanothechnol. **6**, 23 (2010).

[26] P. D. Godwin, S. D. Kenny, and R. Smith, Surf. Sci. **529**, 237 (2003).

[27] J. Y. Lee and M. H. Kang, Surf. Sci. **602**, 1408 (2008).

[28] R. Rurali, R. Cuadrado, and J. I. Cerdà, Phys. Rev. B **81**, 075419 (2010).

[29] S. Yao, C. Zhou, B. Han, T. Fan, J. Wu, L. Chen, and H. Cheng, Phys. Rev. B **79**, 155304 (2009).

[30] D. Chen and D. Sarid, Surf. Sci. **329**, 206 (1995).

[31] H. Wang, C. Zeng, Q. Li, B. Wang, J. Yang, J. G. Hou, and Q. Zhu, Surf. Sci. Lett. **442**, L1024 (1999).

[32] J. I. Pascual, J. Gómez-Herrero, A. Baro, D. Sánchez-Portal, E. Artacho, P. Ordejón, and J. M. Solar, Chem. Phys. Lett. **321**, 78 (2000).

[33] K. Sakamoto, M. Harada, D. Kondo, A. Kimura, A. Kakizaki, and S. Suto, Phys. Rev. B **58**, 13951 (1998).

[34] D. Sánchez-Portal, E. Artacho, J. I. Pascual, J. Gómez-Herrero, R. M. Martin, and J. M. Solar, Surf. Sci. **482-5**, 39 (2001).

[35] G. Baffou, A. J. Mayne, G. Comtet, G. Dujardin, Ph. Sonnet, and L. Stauffer, Appl. Phys. Lett. **91**, 073101 (2007).

[36] H. Yang, O. Boudrioua, A. J. Mayne, G. Comtet, G. Dujardin, Y. Kuk, Ph. Sonnet, L. Stauffer, S. Nagarajan, and A. Gourdon, Phys. Chem. Chem. Phys. **14**, 1700 (2012).

[37] O. Boudrioua, H. Yang, Ph. Sonnet, L. Stauffer, A. J. Mayne, G. Comtet, G. Dujardin, Y. Kuk, S. Nagarajan, A. Gourdon, and E. Duverger, Phys. Rev. B **85**, 035423 (2012).

[38] L. Li, Y. Hasegawa, H. Shinohara, and T. Sakurai, J. Vac. Sci. Technol. B **15**, 1300 (1997).

[39] L. Li, Y. Hasegawa, H. Shinohara, and T. Sakurai, J. Phys. IV **6**, C5-173 (1996).

[40] F. Amy, H. Enriquez, P. Soukiassian, C. Brylinski, A. Mayne, and G. Dujardin, Appl. Phys. Lett. **79**, 767 (2001).

[41] G. Baffou, A. J. Mayne, G. Comtet, and G. Dujardin, Phys. Rev. B **77**, 165320 (2008).

[42] G. Kresse and J. Furthmüller, Phys. Rev. B **54**, 11169 (1996).

[43] J. P. Perdew, J. A. Chevary, S. H. Vosko, K. A. Jackson, M. R. Pederson, D. J. Singh, and C. Fiolhais, Phys. Rev. B **46**, 6671 (1992).

[44] P. E. Blöchl, Phys. Rev. B **50**, 17953 (1994).

[45] G. Kresse and D. Joubert, Phys. Rev. B **59**, 1758 (1999).

[46] S. Grimme, J. Comp. Chem. **25**, 1463 (2004).

[47] S. Grimme, J. Comp. Chem. **27**, 1787 (2006).

[48] S. Grimme, J. Antony, T. Schwabe, and C. Mück-Lichtenfeld, Org. Biomol. Chem. **5**, 741 (2007).

[49] M. Mura, A. Gulans, T. Thonhauser, and L. Kantorovich, Phys. Chem. Chem. Phys. **12**, 4759 (2010).

[50] M.-T. Nguyen, C. A. Pignedoll, M. Treier, R. Fasel, and D. Passerone, Phys. Chem. Chem Phys. **12**, 992 (2010).

[51] D. Künzel, K. Tonigold, J. Kučera, M. Roos, H. E. Hoster, J. Behm, and A. Groß, Chem. Phys. Chem. **12**, 2242 (2011).

[52] F. C. Bocquet, Y. Ksari, L. Giovanelli, L. Porte, and J.-M. Themlin, Phys. Rev. B **84**, 075333 (2011).

[53] A. J. Mayne, C. M. Goringe, C. W. Smith, and G. A. D. Briggs, Surf. Sci. **348**, 209 (1996).

[54] A. J. Mayne, A. R. Avery, J. Knall, T. S. Jones, G. A. D. Briggs, and W. H. Weinberg, Surf. Sci. **284**, 247 (1993).

[55] A. Hemeryck, A. J. Mayne, N. Richard, A. Estève, M. Djafari-Rouhani, Y. J. Chabal, G. Comtet, and G. Dujardin, J. Chem. Phys. **126**, 114707 (2007).

[56] M. Cranney, Y. Chalopin, A. J. Mayne, G. Comtet, and G. Dujardin, Appl. Phys. A **94**, 767 (2009).

[57] W. Feller, *An Introduction to Probability Theory and Its Applications*, Vol. 1 (Wiley, New York, 1966), p. 149.

[58] A. J. Mayne, F. Semond, G. Dujardin, and P. Soukiassian, Phys. Rev. B **57**, 15108 (1998).

[59] G. Dujardin, A. J. Mayne, and F. Rose, Phys. Rev. Lett. **82**, 3448 (1999).